Wind Farm Flow Modeling Using an Input-Output Reduced-Order Model

Jennifer Annoni, Pieter Gebraad, and Peter Seiler

Abstract— **Wind turbines in a wind farm operate individually to maximize their own power regardless of the impact of aerodynamic interactions on neighboring turbines. There is the potential to increase power and reduce overall structural loads by properly coordinating turbines. To perform control design and analysis, a model needs to be of low computational cost, but retains the necessary dynamics seen in high-fidelity models. The objective of this work is to obtain a reduced-order model that represents the full-order flow computed using a high-fidelity model. A variety of methods, including proper orthogonal decomposition and dynamic mode decomposition, can be used to extract the dominant flow structures and obtain a reduced-order model. In this paper, we combine proper orthogonal decomposition with a system identification technique to produce an input-output reduced-order model. This technique is used to construct a reduced-order model of the flow within a two-turbine array computed using a large-eddy simulation.**

I. Introduction

In the United States, many states have a renewable portfolio standard or goal. For example, Minnesota has a renewable portfolio standard target of 25% renewable energy by 2025 [1]. Wind energy will be a significant factor in achieving this goal. Wind farm control can be used to increase wind energy efficiency by maximizing power in wind farms that are already installed. It can also be used to mitigate structural loads to maximize the lifetime of the turbines and better integrate wind energy into the energy market.

Currently, turbines in a wind farm are operated at their individual optimal operating point, which leads to suboptimal performance of the wind farm. Properly coordinating turbines has the potential to increase the overall performance of a wind farm [2]. Designing wind farm control strategies requires a model of the wind farm that has a low computational cost, but retains the necessary dynamics. A variety of wake models exist in literature that are useful for studying wind farm control. The simplest model is the Park model [3], and those that model the wake using a RANS approach with a mixing length model (e.g., the eddy viscosity model [4]). The Park model provides a quick, preliminary description of the wake interactions in a wind farm. Several high-fidelity computational fluid dynamics (CFD) models have been developed as well [5], [6]. These high-fidelity models are more accurate tools and can be used for evaluating wind farm controllers; however, they are computationally expensive. These low- and high-fidelity models have been used to evaluate wind farm control strategies. The analysis provides conflicting results based on the wake model chosen for control design. For example, control strategies designed using simple static models may report significant improvements in wind farm performance, but an analysis of such control strategies using high-fidelity simulations can result in minimal to no improvements in wind farm performance. An example of a comparison between control predictions given by a high-fidelity and simplified model is given in [7], where constant offsets of pitch and torque are used to change wake deficits. It is shown that extensions to the Park model are needed to match the results of high-fidelity models.

Improving models for wind farm control requires a better understanding of the aerodynamic interactions in a wind farm. Although many studies have been performed using static models and constant offsets of the operating point of the wind turbines, dynamic wake modeling and control approaches have been proposed recently. Previously proposed approaches use high-order first principle modeling by implementing the spatially filtered Navier-Stokes equations, e.g., [8], to arrive at a dynamic wake model. This paper focuses on a technique to construct a reduced-order wake model from data generated by simulations or experiments.

Techniques developed by the fluids and controls communities are relevant for reduced-order wake modeling. Some studies have been done to understand the dominant turbulent structures generated in CFD simulations and in experiments [9]. Proper orthogonal decomposition (POD) and dynamic mode decomposition (DMD) are two popular techniques in the fluids literature that compute the dominant modes of the flow. These modes have been used to construct the reduced-order models that can be used for control, such as balanced POD and DMD with control (DMDc) [10]–[13]. Some of these methods require computing the adjoint of the system, which is not readily available in most CFD codes and is not available during experiments. The controls/systems community has an alternative set of techniques to identify models from input-output data, e.g., system identification techniques such as N4SID [14]. The methods generate reduced-order black box models to represent input-output measurements from the system. This type of reduced-order model refers to a low-dimensional representation of a high-dimensional system. In this framework, the states have no physical meaning.

In this paper, we use a method that combines system identification with POD modes that closely follows the DMDc algorithm [13]. This type of model reduction approach has two main advantages. First, it relies on input-output data from a forced response and does not require the construction/simulation of the adjoint system. Second, the

Jennifer Annoni and Peter Seiler are with the Department of Aerospace Engineering & Mechanics, University of Minnesota. anno0010@aem.umn.edu and seiler@aem.umn.edu. Pieter Gebraad (pieter.gebraad@nrel.gov) is with the National Renewable Energy Laboratory (NREL).

reduced-order model is constructed in a way that retains the physical meaning of the states. In other words, the reduced-order state can be mapped back to the approximate full-order state of the system. The method addressed in this paper projects the state onto a reduced-order subspace using the dominant modes of the system and then uses direct N4SID to define the reduced-order model of the system. This paper will begin by reviewing the standard reduced-order modeling techniques in the fluids literature, i.e., POD and DMD, that focus on identifying dominant spatial and temporal modes in the flow of autonomous systems. Next, we will address the method used in this paper to obtain reduced-order models of dynamic systems that include inputs and outputs (Section III). This method has been applied to a high-fidelity CFD simulation of a two-turbine array described in Section IV. The results of obtaining a reduced-order model are presented in Section V. Finally, conclusions and suggestions for future work are given in Section VI.

II. Background: Reduced-order modeling

Two popular methods in the fluids community are addressed in this section. These methods were used in combination with system identification to construct a low-dimensional model from a high-dimensional system.

A. Proper Orthogonal Decomposition

POD provides a low-order approximation of a fluid system that is capable of capturing the dominant structures in the flow. Specifically, POD can be used to extract dominant spatial features from both simulation and experimental data that can be used to uncover the structures in the flow field [15], [16]. This can be done by projecting the velocity field onto a set of orthogonal basis functions.

Consider a system modeled by the following continuous-time nonlinear dynamics:

$$\dot{x}(t) = f(x(t), u(t)) \tag{1}$$

where $x \in \mathbb{R}^n$ is the state vector and $u \in \mathbb{R}^p$ is the input vector. The POD modes of this system can be computed by simulating the system (1) forward in time and collecting snapshots of the nonlinear system, $x(t)$. A data matrix of the snapshots is formed by:

$$X_0 = [x(t_0), x(t_1), ..., x(t_m)] \tag{2}$$

where m is the number of snapshots. The POD modes are then computed by taking the singular value decomposition of the data matrix:

$$X_0 = U\Sigma V^*. \tag{3}$$

The POD modes are contained in the columns of U, and the relative energy of each mode is contained in the singular values in Σ. These modes provide the spatial component of the flow with the first POD mode being the spatial mode that contains the most energy. Note that a reduced-order model can be constructed using POD modes and the Galerkin projection (see [16] for details). In addition, there have been a few other variations of POD that have been developed to directly handle inputs (e.g., [10], [11]). POD modes are good at representing specific data sets; however, they do not necessarily provide a good description of a dynamically evolving flow driven by a forcing input.

B. Dynamic Mode Decomposition

DMD extracts the dominant spatial and temporal information about the flow [17]–[20]. This method attempts to fit a discrete-time linear system to a set of snapshots from simulations or experiments. Consider a system modeled by the following discrete-time nonlinear dynamics:

$$x_{k+1} = f(x_k) \tag{4}$$

where $x \in \mathbb{R}^n$ is the state vector. A collection of snapshot measurements $\{x_k\}_{k=0}^m \in \mathbb{R}^n$ is obtained for the system either via simulations or experiments.

The objective of DMD is to approximate the system on a low-dimensional subspace. Assume there is a matrix A that relates the snapshots in time by:

$$x_{k+1} = Ax_k. \tag{5}$$

The snapshots of the system are defined as:

$$X_0 = [x_0, x_1, ..., x_{m-1}] \tag{6}$$

$$X_1 = [x_1, x_2, ..., x_m] \tag{7}$$

where x_k are the snapshots and m is the number of snapshots. The full-order A matrix can be computed such that:

$$A = X_1 X_0^\dagger \tag{8}$$

where $X_0^\dagger$ indicates the pseudoinverse of X_0. The DMD method attempts to fit the snapshots in time using a low rank matrix that captures the dynamics of the data set. This matrix can be used to construct the DMD modes that correspond to specific temporal frequencies. A low-order representation of x_k can be written as $z_k = Q^* x_k$, where Q is the projection subspace. The truncated, reduced-order model takes the form:

$$z_{k+1} = (Q^* A Q) z_k := F z_k. \tag{9}$$

The state matrix $F := Q^* A Q \in \mathbb{R}^{r \times r}$ describes the dynamics of the reduced-order subspace. Solutions to this reduced-order model can be used to construct the approximate solutions to the full-order model.

The typical choice for the projection subspace, Q, is the POD modes of X_0 (i.e., $Q = U_r$, where r is the order of the reduced-order model). The optimal reduced-order state matrix, F, for this choice is:

$$F := U_r^* A U_r = U_r^* X_1 (U_r^* X_0)^\dagger \tag{10}$$

where the corresponding low rank approximation for the full-order state matrix is:

$$A \approx U_r F U_r^* = U_r U_r^* X_1 X_0^\dagger. \tag{11}$$

If an eigenvalue decomposition is done on F, then A is now:

$$A \approx U_r T \Lambda T^{-1} U_r^* \tag{12}$$

where $U_r T$ are defined as the DMD modes, and the corresponding values of Λ provide the specific temporal frequency for each DMD mode.

One limitation of this approach is that DMD cannot produce input-output models. Specifically, the dynamics and modes will be disrupted by external forcing (i.e., DMD is not robust to perturbations in the system). In addition, this technique is not robust to noise, making it difficult to use for predictive modeling or control. A few studies have been conducted to address this issue [21], [22]. In the studies outlined here, different approaches have been taken to account for noise. In [21], a Kalman filter is used in addition to the reduced-order model obtained using DMD, which helps account for process noise as well as measurement noise. The approach, described in the next section, uses external forcing to identify a reduced-order linear model that is more robust to noise. By introducing an external input, there is a stronger signal-to-noise ratio that is capable of better identifying a reduced-order model.

III. Input-Output Reduced-Order Modeling

In this section, we combine POD with system identification [14], often used in the controls literature, to produce an input-output reduced-order model (IOROM). This term has been used in the aero-servo-elastic flexible aircraft literature [23]. The proposed method closely follows the procedure used in the formulation of DMDc [13]. Specifically, this approach will be summarized in this section for time-invariant systems, but it can be extended to parameter-varying systems [24]. The advantages of using this approach is that it produces input-output models that do not require adjoints and is robust to noise.

Consider a discrete-time nonlinear system with inputs:

$$x_{k+1} = f(x_k, u_k) \tag{13}$$
$$y_k = h(x_k, u_k) \tag{14}$$

where $x \in \mathbb{R}^n$, $u \in \mathbb{R}^p$, and $y \in \mathbb{R}^q$ are the state, input, and output vectors.

A collection of snapshot measurements are obtained via simulations or experiments by exciting the system. Snapshots are taken from the nonlinear system, and the states (similar to DMD), inputs, and outputs are recorded as:

$$X_0 = [x_1, x_2, ..., x_{m-1}] \tag{15}$$
$$X_1 = [x_2, x_3, ..., x_m] \tag{16}$$
$$U_0 = [u_1, u_2, ..., u_{m-1}] \tag{17}$$
$$Y_0 = [y_1, y_2, ..., y_{m-1}]. \tag{18}$$

This method attempts to fit the snapshot measurements at a particular operating point in time by:

$$x_{k+1} = Ax_k + Bu_k \tag{19}$$
$$y_k = Cx_k + Du_k. \tag{20}$$

The dimensions of the state matrices (A, B, C, D) are compatible to those of (x, u, y). The state is projected onto a low-dimensional subspace to make the computations tractable.

A truncated model can be expressed in terms of this reduced-order state (i.e., $z = Q^* x \in \mathbb{R}^r$, where $Q \in \mathbb{R}^{n \times r}$ is a generic orthonormal basis that forms the projection subspace).

$$z_{k+1} = (Q^* A Q) z_k + (Q^* B) u_k := F z_k + G u_k \tag{21}$$
$$y_k = (CQ) z_k + D u_k := H z_k + D u_k \tag{22}$$

The reduced-order state matrices (F, G, H, D) are obtained by minimizing the error of the Frobenius norm using least-squares:

$$\min_{\left[\begin{smallmatrix} F & G \\ H & D \end{smallmatrix}\right]} \left\| \begin{bmatrix} X_1 \\ Y_1 \end{bmatrix} - \begin{bmatrix} Q & 0 \\ 0 & I \end{bmatrix} \begin{bmatrix} F & G \\ H & D \end{bmatrix} \begin{bmatrix} Q^* & 0 \\ 0 & I \end{bmatrix} \begin{bmatrix} X_0 \\ U_0 \end{bmatrix} \right\|_F^2. \tag{23}$$

This is the direct N4SID subspace method for estimating state matrices given measurements of the (reduced-order) state, input, and output. A useful choice for the projection space is given by the POD modes of X_0; see (3). The state of the linear system can be approximated on a subspace defined by the first r POD modes of X_0. The optimal reduced-order state matrices for this choice are:

$$\begin{bmatrix} F & G \\ H & D \end{bmatrix}_{opt} = \begin{bmatrix} U_r^* X_1 \\ Y_0 \end{bmatrix} \begin{bmatrix} \Sigma_r V_r \\ U_0 \end{bmatrix}^\dagger. \tag{24}$$

As with standard DMD, an eigenvalue decomposition of F_{opt} can be used to construct these modes, which provide spatial modes associated with a specific temporal frequency for the system. It should be noted that the F matrices obtained in DMD and this approach should be the same. The F matrix describes the dynamics of the system. As mentioned previously, DMD is often not robust to sensor or process noise, and it does not handle inputs and outputs, which is necessary for the wind farm problem. The G, H, and D matrices obtained using this method are computed such that the input-to-output relationship of the reduced-order model is maintained from the full-order system. This proposed method is a tractable implementation of the existing direct N4SID (subspace) method [14] that can be applied for very large systems. This is not simply a black-box (input-output) approach because the state of the reduced-order system z_k can be used to approximately reconstruct the full-order state by:

$$x_k \approx U_r z_k. \tag{25}$$

Moreover, the approach only requires input/output/state data from the model. Construction and simulation of an adjoint system is not required.

IV. Simulation Setup

The IOROM method described in Section III was used to obtain a reduced-order model from the Simulator fOr Wind Farm Applications (SOWFA) simulations. The goal of this study is to construct a reduced-order model that can be used to reconstruct the dominant characteristics of the flow field seen in high-fidelity models.

A. Simulator fOr Wind Farm Applications

SOWFA is a high-fidelity large eddy simulation tool that was developed at the National Renewable Energy Laboratory (NREL) for wind farm studies. SOWFA is a CFD solver based on OpenFOAM that is coupled with NREL's FAST modeling tool. SOWFA has been used in previous wind farm control studies [5], [25], [26].

SOWFA uses an actuator line model coupled with FAST to study turbines in the atmospheric boundary layer. Specifically, SOWFA solves the three-dimensional incompressible Navier-Stokes equations and transport of potential temperature equations, which take into account the thermal buoyancy and Earth rotation (Coriolis) effects in the atmosphere. The inflow conditions for this simulation are generated using a periodic atmospheric boundary layer precursor with no turbines. Additional details can be found in [26].

SOWFA calculates the unsteady flow field to compute the time-varying power, velocity deficits, and loads at each turbine in a wind farm. This level of computation, with high-fidelity accuracy, takes a number of days to run on a supercomputer using a few hundred to a few thousand processors, depending on the size of the wind farm. The simulations run for this study were performed on NREL's high-performance computer Peregrine.

B. Two-Turbine Setup

A high-fidelity simulation of a two-turbine scenario was performed with SOWFA to provide the data for the IOROM. The turbines were aligned with a spacing of 5 D. The simulated turbines are NREL 5-MW baseline turbines [27], which have a rotor diameter of D = 126 m. Details about the positioning of the turbines in the domain are given in Fig. 1. The spatial discretization for CFD is refined in two steps in a rectangular region, with the smallest cells containing the turbine rotors, the axial-induction zones of the rotor, and a large part of the wake. Farther from the turbines, the mesh is coarser to reduce computation time.

The conditions simulated in SOWFA are based on the study reported in [25], [26]. They consist of a neutral atmospheric boundary layer with a low aerodynamic surface roughness value of 0.001 m, which is typical for offshore conditions. The generated inflow, coming from the southwest (300°), has a horizontally averaged wind speed of 8 m/s and a turbulence intensity of 10% at the turbine hub height. We used a simulation time of 1800 s to let the wakes develop through the domain.

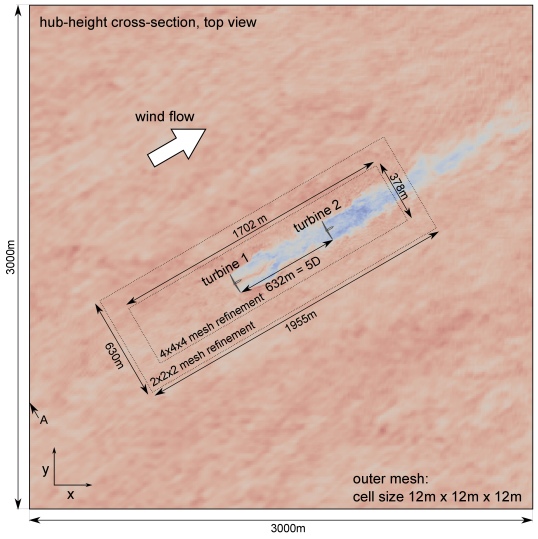

Fig. 1. Setup for the two-turbine array in SOWFA.

C. IOROM from SOWFA

A forced input was applied to the upstream turbine by changing the collective blade pitch angle from 0° to 4° using a pseudorandom binary sequence; see Fig. 2. The corresponding power output for each turbine is shown in the bottom plot of Fig. 2. This indicates how the forcing input at the upstream turbine affects the power output of both the upstream and the downstream turbine. By changing the blade pitch from 0° to 4° at varying frequencies, various dynamics of the system are excited. This help accurately identify a reduced-order model of this system.

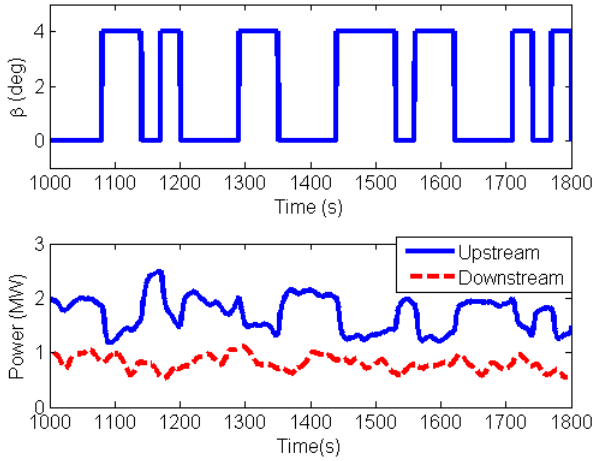

Fig. 2. Forced input used for the two-turbine array.

The data from the simulations were sampled at 1 s intervals (i.e., snapshots of the flow are recorded every 1 s). The sampling time was determined by doing a frequency analysis of the flow in a two-turbine array. In particular, Fig. 3 shows the frequency content within a wake 4 D downstream of the upstream turbine. In addition, Fig. 3

shows that a majority of the frequency content in the rotor-swept area (63 m around the origin) of the wake does not exceed 0.5 Hz. There is a higher frequency at the edge of the wake because of the presence of a shear layer. For this analysis, it should be noted that the fast Fourier transform in Fig. 3 is based on 1 Hz data. The Nyquist frequency is thus 0.5 Hz. We see that in the wake, the variation is not higher than 0.5 Hz. It should also be noted that the time step of interest for this particular method is the sampling rate, 1 s, rather than the time scale of the CFD solver. As a result, it was determined that we do not need higher frequency data to do this analysis. The inputs of interest for this problem are the blade pitch angle of the upstream turbine, the generator torque of the upstream turbine, and the generator torque of the downstream turbine. The outputs of interest include the power from the upstream turbine and the power from the downstream turbine. The purpose of this model is to be able to approximately reconstruct the flow corresponding to these inputs and outputs.

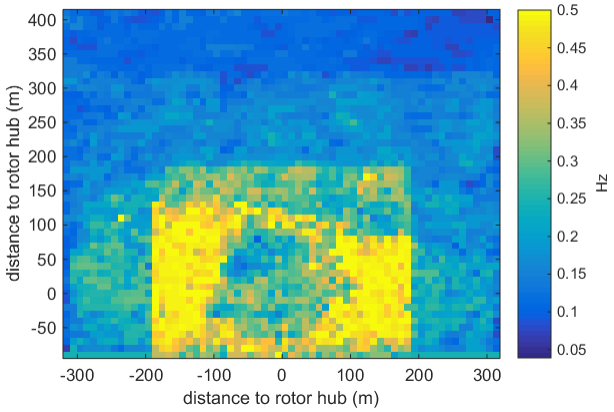

Fig. 3. Frequency content of the flow velocity field at 4 D downstream of the upstream turbine. Specifically, this shows the -20 dB bandwidth of the fast Fourier transform of the velocity signal for sample points at 4 D downstream. Note that the velocity signal was sampled at 1 Hz. The pure yellow may indicate that the frequency at these points exceeds 0.5 Hz.

V. Results

The results shown in this section were obtained using the IOROM method described in Section III on the simulation scenarios described in Section IV-B. Note that the resulting flow fields have been rotated in this section so that the flow is shown moving from left to right. The upstream and downstream turbines are indicated by black lines in the figures in this section. In particular, we will focus on reconstructing the flow (i.e., the state evolution equation $x_{k+1} = Ax_k + Bu_k$, where x is the flow velocity at the sampled grid points, $u := [\beta_1, \tau_{g1}, \tau_{g2}]$, where β_1 is the blade pitch angle at the upstream turbine, and τ_{g1} and τ_{g2} are the generator torques at the upstream and downstream turbines, respectively). The blade pitch angle at the downstream turbine is zero in this example and is excluded from the inputs. These inputs are associated with the force that the turbines are applying to the flow and are essential to include in the reduced-order model. For this particular example, there are approximately 1.2 million sampled grid points and the three velocity components are recorded at each grid point. Hence, the dimension of x is approximately 3.6 million. It should be noted that this paper is primarily focused on reconstructing the flow field x (i.e., the states). In particular, this approach can be used to find a low-order representation of the system where the states have physical meaning. This is useful when applying this method to linear parameter-varying systems [24]. When obtaining an input-output model for this system, a typical output used with this approach would be the power output of each turbine or the wind speed directly in front of each turbine (approximately 1 D upstream of the turbine). Future results will address the input-to-output relationship.

The POD modes of the simulation were computed using the MapReduce approach [28]. Specifically, we used 800 snapshots at 1 s intervals for a total time of 800 s to compute the POD modes of the system. This indicates that the lowest frequency that we could capture with the reduced-order model constructed in this paper is on the order of 10^{-2}. Fig. 4 shows the POD modes 1, 2, 10, 20, 50, and 100 of the streamwise velocity component at hub height (90 m). As described in Section III, the POD modes are used to project the system on to a low-dimensional subspace such that direct N4SID can be used to identify a low-order model of the high-dimensional system. It should be noted that these modes were computed after subtracting out the baseflow (i.e., the mean flow). The first mode contains low-frequency spatial information and is the most energetic mode of the system. Mode 100 has high-frequency spatial information and represents a small amount of energy in the system.

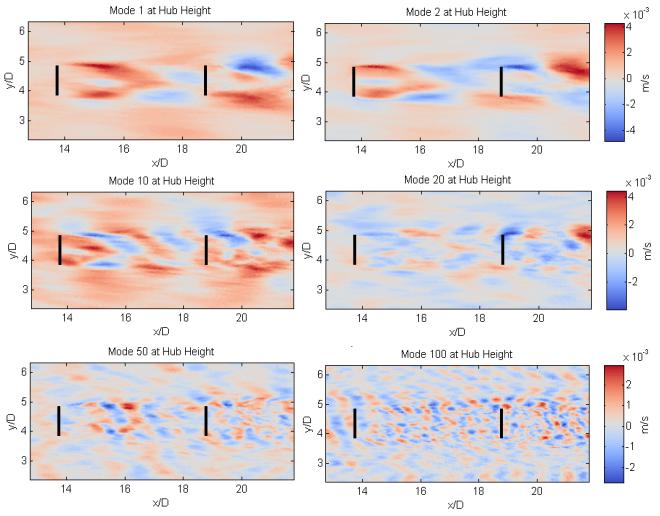

Fig. 4. Modes 1, 2, 10, 20, 50, and 100 of the two-turbine array. Note: the plots are in m/s.

The full flow field is computed from the results of the reduced-order model using (25) and is shown in Fig. 5. The bottom plot of Fig. 5 indicates the blade pitch angle at the upstream turbine and the dot indicates the blade pitch angle of the instantaneous snapshot represented in the top three

plots. For this reconstruction, we selected 20 modes and specifically looked at the streamwise velocity component at hub height. By only selecting 20 modes, this reduced-order model will not be able to capture the high-frequency spatial turbulence. The order of this model was selected by evaluating the mean error accumulated when comparing the SOWFA flow field with the reduced-order flow field. It is important to note that if too many modes are selected, then the model will try to overfit to the turbulence rather than the dominant dynamics of the system.

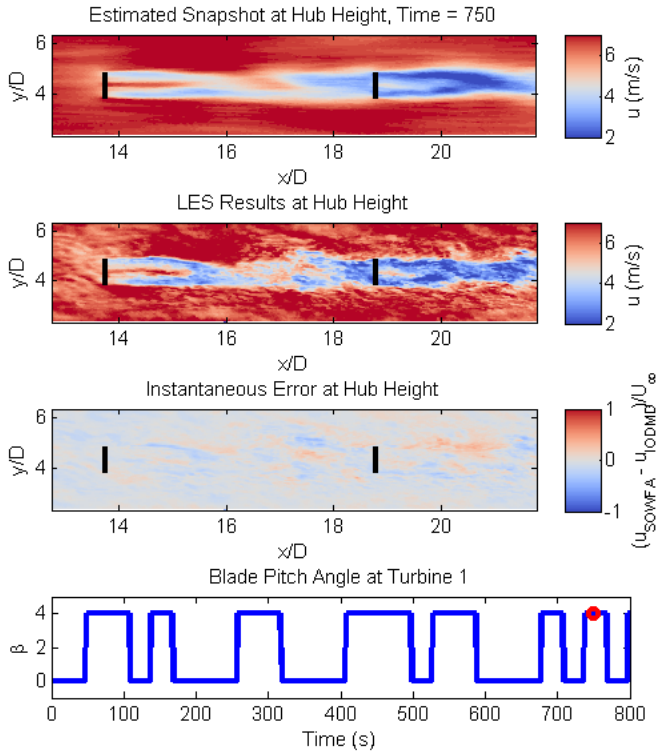

Fig. 5. Flow reconstructed using the reduced-order model (top) and compared to SOWFA (middle). The bottom plot indicates the blade pitch angle at the upstream turbine.

Lastly, this model was applied to a set of validation data to verify that it would work under similar wind conditions but with a different forced input. The same inflow fields were used for the training and validation cases. Additional work is being done to understand the effects of using different inflow conditions. The same model that was used to construct Fig. 5 is used to reconstruct the flow for the validation data. Fig. 6 shows that this model is able to similarly reconstruct the dominant characteristics of the flow provided in the validation case. The results in Fig. 6 indicate that a reduced-order model has been obtained using the proposed approach and can be used as a predictive model for another similar data set. The time-averaged error between SOWFA and the reduced-order model in the validation case is shown in Fig. 7. The time-averaged error is an average of the instantaneous error snapshots (i.e., the third plot in Fig. 7). Specifically, the instantaneous error is determined by subtracting streamwise velocity obtained from the reduced-order model from the streamwise velocity computed in SOWFA. The maximum error occurs on the edges of the wakes and may be a result of excess mixing far downstream (4 D) of the upstream turbine; however, this error is less than 10%. Fig. 6 further demonstrates that the reduced-order model is able to capture a majority of the flow characteristics by comparing the streamwise velocity computed in SOWFA and in the IOROM.

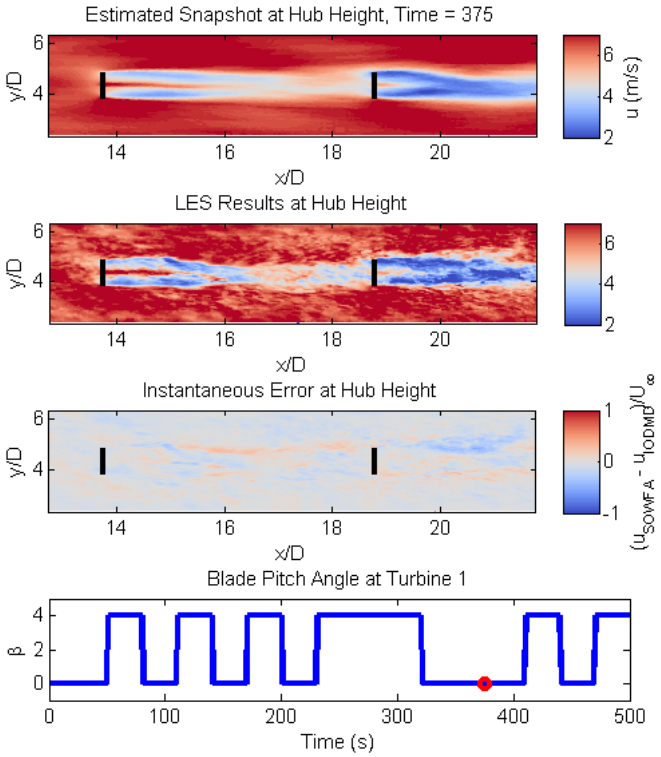

Fig. 6. Flow reconstructed for the validation case using the reduced-order model (top) and compared to SOWFA (middle). The bottom plot indicates the blade pitch angle at the upstream turbine.

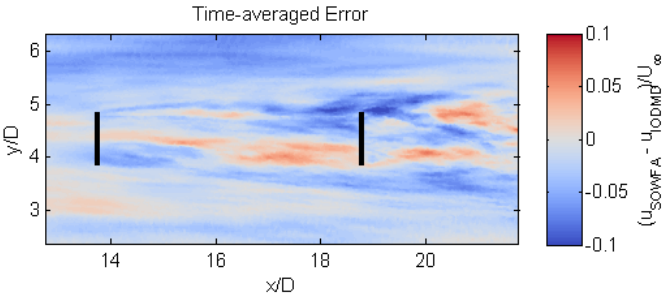

Fig. 7. Time-averaged error of the validation data.

VI. Conclusions and Future Work

This paper describes a method that combines POD and system identification to construct an IOROM. The application of this method was a high-fidelity wake model, SOWFA. We were able to identify a 20-state model that can reconstruct

the dominant characteristics of the flow. Future work will include constructing a reduced-order model from SOWFA using this approach to design and analyze a closed-loop controller that can be used for wind farm control in high-fidelity simulations.

VII. Acknowledgments

This work was supported by the National Science Foundation under Grant No. NSF-CMMI-1254129 entitled CAREER: Probabilistic Tools for High Reliability Monitoring and Control of Wind Farms.

The first author gratefully acknowledges the financial support from University of Minnesota through the 2015-16 Doctoral Dissertation Fellowship.

Lastly, this work was supported by the U.S. Department of Energy under Contract No. DE-AC36-08GO28308 with the National Renewable Energy Laboratory. Funding for the work was provided by the DOE Office of Energy Efficiency and Renewable Energy, Wind and Water Power Technologies Office. The authors are solely responsible for any omission or errors contained herein.

References

[1] R. Wiser, "Renewable portfolio standards in the United States - a status report with data through 2007," LBNL-154E, Lawrence Berkeley National Laboratory, 2008.

[2] K. E. Johnson and N. Thomas, "Wind farm control: Addressing the aerodynamic interaction among wind turbines," in *American Control Conference*, pp. 2104–2109, 2009.

[3] N. O. Jensen, "A note on wind generator interaction," Tech. Rep. Risø-M-2411, Risø, 1983.

[4] J. F. Ainslie, "Calculating the flowfield in the wake of wind turbines," *Journal of Wind Engineering and Industrial Aerodynamics*, vol. 27, no. 1, pp. 213–224, 1988.

[5] M. Churchfield and S. Lee, "NWTC design codes-SOWFA," `https://nwtc.nrel.gov/SOWFA`, 2012.

[6] X. Yang and F. Sotiropoulos, "On the predictive capabilities of les-actuator disk model in simulating turbulence past wind turbines and farms," in *American Control Conference*, pp. 2878–2883, 2013.

[7] J. Annoni, P. M. Gebraad, A. K. Scholbrock, P. A. Fleming, and J.-W. v. Wingerden, "Analysis of axial-induction-based wind plant control using an engineering and a high-order wind plant model," *Wind Energy*, 2015.

[8] J. P. Goit and J. Meyers, "Optimal control of energy extraction in wind-farm boundary layers," *Journal of Fluid Mechanics*, vol. 768, pp. 5–50, 2015.

[9] D. Bastine, B. Witha, M. Wächter, and J. Peinke, "Towards a simplified dynamic wake model using POD analysis," *arXiv preprint arXiv:1409.1150*, 2014.

[10] C. Rowley, "Model reduction for fluids, using balanced proper orthogonal decomposition," *International Journal of Bifurcation and Chaos*, vol. 15, no. 03, pp. 997–1013, 2005.

[11] K. Willcox and J. Peraire, "Balanced model reduction via the proper orthogonal decomposition," *AIAA journal*, vol. 40, no. 11, pp. 2323–2330, 2002.

[12] M. Balajewicz, *A New Approach to Model Order Reduction of the Navier-Stokes Equations*. PhD thesis, Duke University, 2012.

[13] J. L. Proctor, S. L. Brunton, and J. N. Kutz, "Dynamic mode decomposition with control," *arXiv preprint arXiv:1409.6358*, 2014.

[14] M. Viberg, "Subspace-based methods for the identification of linear time-invariant systems," *Automatica*, vol. 31, no. 12, pp. 1835–1851, 1995.

[15] J. L. Lumley, *Stochastic tools in turbulence*. Courier Corporation, 2007.

[16] P. Holmes, J. L. Lumley, and G. Berkooz, *Turbulence, coherent structures, dynamical systems and symmetry*. Cambridge University Press, 1998.

[17] P. J. Schmid, "Dynamic mode decomposition of numerical and experimental data," *Journal of Fluid Mechanics*, vol. 656, pp. 5–28, 2010.

[18] I. Mezić, "Spectral properties of dynamical systems, model reduction and decompositions," *Nonlinear Dynamics*, vol. 41, no. 1-3, pp. 309–325, 2005.

[19] K. K. Chen, J. H. Tu, and C. W. Rowley, "Variants of dynamic mode decomposition: boundary condition, Koopman, and Fourier analyses," *Journal of Nonlinear Science*, vol. 22, no. 6, pp. 887–915, 2012.

[20] P. J. Schmid, L. Li, M. Juniper, and O. Pust, "Applications of the dynamic mode decomposition," *Theoretical and Computational Fluid Dynamics*, vol. 25, no. 1-4, pp. 249–259, 2011.

[21] G. Iungo, C. Santoni-Ortiz, M. Abkar, F. Porté-Agel, M. Rotea, and S. Leonardi, "Data-driven reduced order model for prediction of wind turbine wakes," in *Journal of Physics: Conference Series*, vol. 625, p. 012009, IOP Publishing, 2015.

[22] S. Dawson, M. Hemati, M. Williams, and C. Rowley, "Characterizing and correcting for the effect of sensor noise in the dynamic mode decomposition," *Bulletin of the American Physical Society*, vol. 59, 2014.

[23] B. Danowsky, T. Lieu, and A. Coderre-Chabot, "Control oriented aeroservoelastic modeling of a small flexible aircraft using computational fluid dynamics and computational structural dynamics," in *Proceedings of the AIAA SciTech Conference, San Diego, CA*, 2016.

[24] J. Annoni and P. Seiler, "A method to construct reduced-order parameter varying models," *Submitted to International Journal of Robust and Nonlinear Control*, 2015.

[25] P. Fleming, P. M. Gebraad, S. Lee, J.-W. Wingerden, K. Johnson, M. Churchfield, J. Michalakes, P. Spalart, and P. Moriarty, "Simulation comparison of wake mitigation control strategies for a two-turbine case," *Wind Energy*, 2014.

[26] P. A. Fleming, P. M. Gebraad, S. Lee, J.-W. van Wingerden, K. Johnson, M. Churchfield, J. Michalakes, P. Spalart, and P. Moriarty, "Evaluating techniques for redirecting turbine wakes using SOWFA," *Renewable Energy*, vol. 70, pp. 211–218, 2014.

[27] J. M. Jonkman, S. Butterfield, W. Musial, and G. Scott, *Definition of a 5-MW reference wind turbine for offshore system development*. National Renewable Energy Laboratory Golden, CO, 2009.

[28] J. Dean and S. Ghemawat, "MapReduce: simplified data processing on large clusters," *Communications of the ACM*, vol. 51, no. 1, pp. 107–113, 2008.